AGU PUBLICATIONS

Geophysical Research Letters

RESEARCH LETTER
10.1002/2015GL064583

Key Points:
- PMIP3 models show an increase in transport and deepening of the AMOC in the LGM
- This result contradicts some observations from proxy data in sediments
- A circulation model indicates that the increment may be due to wind stress

Supporting Information:
- Supporting Information S1

Correspondence to:
J. Muglia,
jmuglia@coas.oregonstate.edu

Citation:
Muglia, J., and A. Schmittner (2015), Glacial Atlantic overturning increased by wind stress in climate models, *Geophys. Res. Lett.*, *42*, doi:10.1002/2015GL064583.

Received 12 AUG 2015
Accepted 27 OCT 2015
Accepted article online 30 OCT 2015

Glacial Atlantic overturning increased by wind stress in climate models

Juan Muglia[1] and Andreas Schmittner[1]

[1]College of Earth, Ocean, and Atmospheric Sciences, Oregon State University, Corvallis, Oregon, USA

Abstract Previous Paleoclimate Model Intercomparison Project (PMIP) simulations of the Last Glacial Maximum (LGM) Atlantic Meridional Overturning Circulation (AMOC) showed dissimilar results on transports and structure. Here we analyze the most recent PMIP3 models, which show a consistent increase (on average by $41 \pm 26\%$) and deepening (663 ± 550 m) of the AMOC with respect to preindustrial simulations, in contrast to some reconstructions from proxy data. Simulations run with the University of Victoria (UVic) ocean circulation model suggest that this is caused by changes in the Northern Hemisphere wind stress, brought about by the presence of ice sheets over North America in the LGM. When forced with LGM wind stress anomalies from PMIP3 models, the UVic model responds with an increase of the northward salt transport in the North Atlantic, which strengthens North Atlantic Deep Water formation and the AMOC. These results improve our understanding of the LGM AMOC's driving forces and suggest that some ocean mechanisms may not be correctly represented in PMIP3 models or some proxy data may need reinterpretation.

1. Introduction

The Atlantic Meridional Overturning Circulation (AMOC) is a part of the climate system, important for understanding the dynamics of the ocean in a past scenario such as the Last Glacial Maximum (LGM, 26–19 kyr before present [*Clark et al.*, 2009]). It is an indicator of the transport and ventilation rates of the deep ocean and plays an important role in biogeochemical cycles and the climate of northwestern Europe. It is thought to be driven by a variety of processes, such as wind stress, buoyancy fluxes, and mixing [*Kuhlbrodt et al.*, 2007]. The AMOC can be described by using the meridional stream function $\psi(y, z)$, which is the zonally and depth-integrated meridional velocity in the Atlantic Ocean and has units of volume transport, usually reported in sverdrups ($1\ \mathrm{Sv} = 10^6 \mathrm{m}^3/\mathrm{s}$).

Reconstructions from sediment cores indicate differences between the modern and LGM AMOC. Benthic foraminifera δ^{18}O data suggest a weaker transport of the Gulf Stream [*Lynch-Stieglitz et al.*, 1999] that would make for a weaker AMOC than today's. Some $^{231}\mathrm{Pa}/^{230}\mathrm{Th}$ records in the Atlantic Basin [*McManus et al.*, 2004] have been interpreted as a weaker AMOC during the LGM, while other studies [e.g., *Gherardi et al.*, 2009] suggest a stronger and shallower circulation. The distribution of δ^{13}C reconstructed from benthic foraminifera implies a similar AMOC but shallower North Atlantic Deep Water (NADW) [*Gebbie*, 2014]. Pore water measurements in sediments show that bottom water temperatures were close to freezing point and that Antarctic Bottom Water (AABW) had higher salinity than NADW [*Adkins et al.*, 2002].

The Paleoclimate Model Intercomparison Project Phase 3 (PMIP3), a joint effort of different coupled ocean-atmosphere general circulation models to simulate the LGM [*Braconnot et al.*, 2012], provides an opportunity to test models that are used for climate projections [*Stocker et al.*, 2013]. The PMIP3 experimental design uses prescribed LGM values for orbital parameters, trace gases, and ice sheets. Sea level drop is considered in the land-sea masks and background salinities of all models, and bathymetry changes in some of them. Ocean currents, temperature, salinity, and other variables are calculated by the models.

The previous version of PMIP (PMIP2) showed dissimilar results between the simulated ocean state of the LGM. Some models predicted a slower and shallower AMOC, while others predicted it as deeper and stronger [*Otto-Bliesner et al.*, 2007]. At the same time, relative changes in temperature and salinity between AABW and NADW were different among models. *Weber et al.* [2007] suggest that the density difference between AABW and NADW controls the AMOC in PMIP2 models, but they did not consider changes in wind stress.

Here we study the AMOC as simulated by PMIP3 models, in their preindustrial control (PIC) and LGM ensembles. We compare simulations to observations, study the changes between the periods, and try to understand which processes control these changes in the models.

Coupled ocean-atmospheric models show that a higher ice sheet over North America results in a stronger AMOC [*Ullman et al.*, 2014; *Zhang et al.*, 2014]. However, the precise process governing this response, which may be changes in atmospheric circulation, hydrological cycle and buoyancy fluxes, or wind stress, remains unknown.

Among the drivers of the AMOC, wind stress $\tau = (\tau_x, \tau_y)$ plays an important role. It affects the strength of surface currents (e.g., the Gulf Stream), the meridional salt transport, and the upwelling of deep waters in the Southern Hemisphere, which have been suggested to impact the AMOC [*Toggweiler and Samuels*, 1995]. From ocean models, *Montoya and Levermann* [2008], *Oka et al.* [2012], and *Wunsch* [2003] have suggested that stronger LGM winds could have increased the AMOC. Here we quantify wind stress effects on the AMOC and its role in the LGM circulation of the PMIP3 models.

2. Materials and Methods

Values of 50-year time-averaged Atlantic meridional stream function $\psi(y, z)$ were obtained from eight PMIP3 models. To quantify the effect of wind stress on the AMOC, we conducted sensitivity experiments with the University of Victoria (UVic) Earth System Climate Model version 2.9 [*Weaver et al.*, 2001]. This model includes a three-dimensional dynamical ocean with 19 vertical levels at $3.6^\circ \times 1.8^\circ$ horizontal resolution governed by the primitive equations, coupled to a two-dimensional single-level atmosphere, with moisture and heat balances and fluxes between the two mediums, and a dynamical sea ice model. Wind stress, wind used in moisture advection, and air-sea fluxes as well as clouds are prescribed from a present-day monthly climatology. Diapycnal mixing is calculated with a three-dimensional parametrization that simulates tide effects [*Schmittner and Egbert*, 2013].

For the sensitivity experiments, we calculated LGM anomalies (LGM minus PIC) of wind stress from the output of the PMIP3 models (Figure S1 in the supporting information). The LGM anomalies were added to present-day fields from the National Centers for Environmental Prediction (NCEP) reanalysis [*Kalnay et al.*, 1996] and used as surface momentum forcing of the ocean and sea ice in the UVic model. We preformed a different run for each PMIP3 model. Results are compared to a default run with no anomalies added. We also performed experiments with anomalies from four PMIP2 models for which pertinent output was available.

Atmospheric CO_2 was set to 185 ppm, with orbital parameters corresponding to 21 kyr. Average salinities were not adjusted for lower than present sea level. We do not focus here on the effects of a globally uniform increase in salinity.

We used continental ice sheet height and fraction from two different reconstructions: ICE-4G [*Peltier*, 1994] and the ice sheet that PMIP3 models use, which is a blend of three other reconstructions [*Abe-Ouchi et al.*, 2015]. For the experiments with PMIP2 wind stress anomalies, we used ICE-5G [*Peltier*, 2004], used in that version of the intercomparison project [*Braconnot et al.*, 2007]. In Figure S2 we show the ice thickness and fraction of all the ice reconstructions, regridded to our model's grid.

A modern distribution of river basins was used. Changing the river routing in North America to account for the Laurentide Ice Sheet did not produce significant changes in the ocean circulation (Figure S3).

For each case, the UVic model was run for 2000 years. Results from the last 500 years are presented.

3. Results

3.1. AMOC as Simulated by PMIP3 Models

In Figure 1 (top row), the upper cell of the AMOC (to which we will simply refer as AMOC) can be distinguished as the zone with positive values of ψ in the upper ~2500 m of the water column, spanning from ~30°S to ~60°N.

The multimodel average PIC AMOC value at 25°N is 16.48 ± 3.67 Sv, with uncertainties defined as the 1σ standard deviation among models. This number is in agreement with modern measurement-based estimates of 17.2 Sv [*McCarthy et al.*, 2015]. Inflow of Circumpolar Deep Water (CPDW) into the Indo-Pacific (IP) is generally lower (8.6 ± 3.6 Sv at 32°S) than modern observations of 14.9 Sv [*McCarthy et al.*, 2015]. This

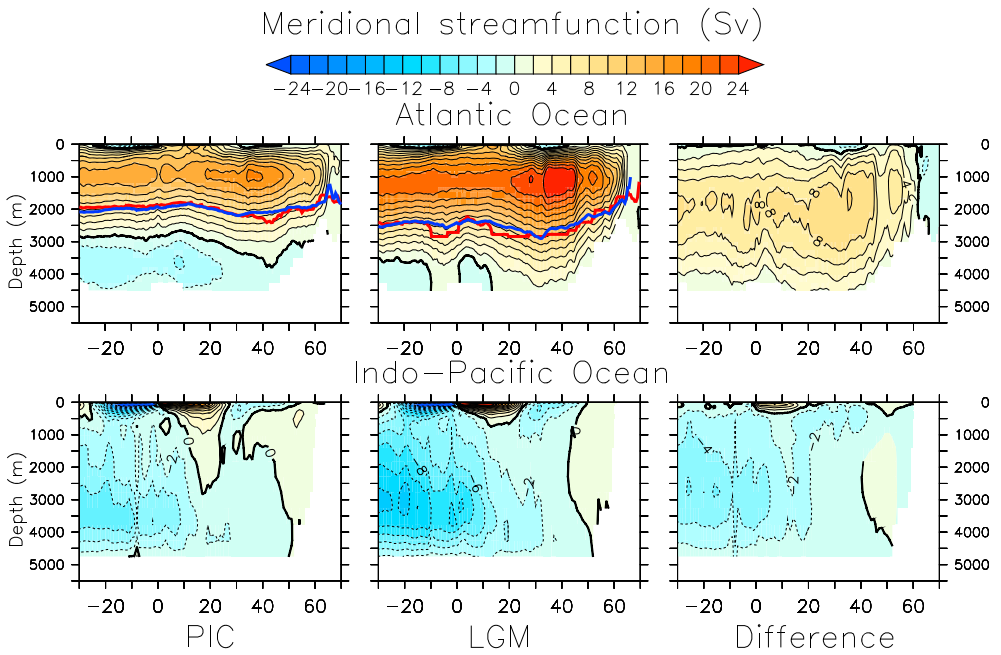

Figure 1. Multimodel mean of Atlantic and Indo-Pacific meridional stream function $\psi(y,z)$ calculated by PMIP3 models. Abscissa axes are in °N. First column corresponds to PIC simulations, second column corresponds to LGM simulations, and third column corresponds to the difference. Isoline difference is 2 Sv. In the Atlantic plots, the red line is the depth of the AMOC calculated as the middle depth between $\psi = \psi_{max}$ and $\psi = 0$, and the blue line is the depth where $\psi = \psi_{max}/2$. Positive (negative) values correspond to clockwise (anticlockwise) circulation.

suggests that AABW formation mechanisms are not correctly represented by the models and/or that diapycnal mixing or geothermal heat fluxes are underestimated in the abyssal IP.

PMIP3 models show stronger AMOC transport during the LGM (see Figure 1 for the multimodel mean and Figure S4 for each individual model). In most models, the upper clockwise cell reaches deeper in the LGM simulations, suggesting a deeper NADW. Community Climate System Model version 4 (CCSM4) shows a shallowing of NADW and increased penetration of AABW in the North Atlantic (NA).

In CCSM4 and in the Goddard Institute for Space Studies model (GISS) the AABW cell is intensified; Max-Planck-Institut model (MPI) shows little change, whereas in the five other models the deepening of the NADW cell weakens AABW and pushes it south. Inflow of CPDW into the IP increases by ∼5 Sv (Figures 1 and S5), suggesting that the enhanced NADW flow into the Southern Ocean (SO) contributes to more CPDW flow into the IP.

The LGM multimodel mean of maximum transport of the AMOC at 25°N is 23 ± 3 Sv, a (41± 26)% average increase when compared to PIC (Table 1). This strengthening is in contrast with reconstructions of a weaker LGM AMOC [*Lynch-Stieglitz et al.*, 2007; *McManus et al.*, 2004]. It is in closer agreement with reconstructions that indicate a stronger AMOC, like *Lippold et al.* [2012] or *Gherardi et al.* [2009], although the latter suggests a shallower AMOC.

The NADW depth was estimated in two ways: as the depth at which ψ was one half of its maximum value and as the middle depth between the maximum ψ and $\psi = 0$ isolines. Both estimates give similar values (Figure 1). We obtained, on average, 2069 m for the PIC and 2732 m for the LGM (32% of increment, Table 1). This contrasts with estimates of an LGM NADW between 0 and 1000 m shallower, based on an inverse model solution using carbon and oxygen isotope reconstructions from LGM sediments [*Gebbie*, 2014].

Concerning bottom temperatures and salinity, PMIP3 PIC simulations are in fair agreement with observations (Figure 2). However, LGM simulations are in disagreement with reconstructions from sediment pore water estimates [*Adkins et al.*, 2002]. NA bottom waters are too warm, whereas SO and South Pacific are too fresh in the models. None of the models predict saltier AABW than NADW or bottom water potential temperatures below −1°C. This is in contrast to PMIP2, where two models (CCSM3 and Hadley Centre Coupled Model (HADCM3)) showed results more in line with Adkins' estimates.

Table 1. Maximum Transport and Depth of the AMOC at 25°N Calculated by PMIP3 Models, in Their PIC and LGM Simulations, and Percentage of Increment Between the Two Periods[a]

Model	PIC (Sv)	LGM (Sv)	Change (%)	PIC Depth (m)	LGM Depth (m)	Change (%)
CCSM4	19.69	21.53	9	2608	2333	−10
GISS	16.92	22.32	32	2055	2273	11
CNRM	13.03	22.74	74	1735	3230	86
MPI	18.19	21.37	17	1963	1993	01
MIROC	13.56	22.07	63	1795	2745	53
MRI	14.82	21.76	47	2193	3363	53
FGOALS	23.02	31.64	37	1965	2940	50
IPSL	12.64	23.04	82	2238	2980	78
Mean	16.48	23.31	41	2069	2732	32

[a]Bottom row is the multimodel mean.

3.2. Sensitivity Experiments With the UVic Model

In the default LGM case with modern winds and PMIP3 ice sheets (Figure 3, top row), UVic model's AMOC is weaker (9.10 Sv at 25°N) and shallower (1900 m if calculated by the method used in the previous section) than in the preindustrial case (15.78 Sv, 2030 m, Figure S6). Since the wind stress is identical in both LGM and PIC cases, we deduce that this response is caused by changes in surface buoyancy forcing.

An LGM simulation with modern winds and ICE-4G ice sheets produces a collapsed AMOC. When PMIP3 LGM wind stress anomalies are applied, the AMOC increases for all model cases, producing stable solutions with a transport of (14.82 ± 1.59) Sv at 25°N (Figure 3). This type of behavior of climate models has been previously documented by *Oka et al.* [2012].

When using PMIP3 LGM wind stress anomalies and continental ice sheets, the average AMOC at 25°N is (12.67 ± 1.10) Sv (Table 2 and Figures 3 and S7). This is (39 ± 11)% stronger than the default case with the same ice sheets. Average depth of the AMOC at 25°N is 3000 m. This represents an increment of approximately 54% with respect to the default run. Inflow of Circumpolar Deep Water (CDW) is intensified by ~1 Sv in the IP, whereas AABW flow into the Atlantic is weakened. These changes are consistent, at least qualitatively, with the response of the PMIP3 models to LGM boundary conditions.

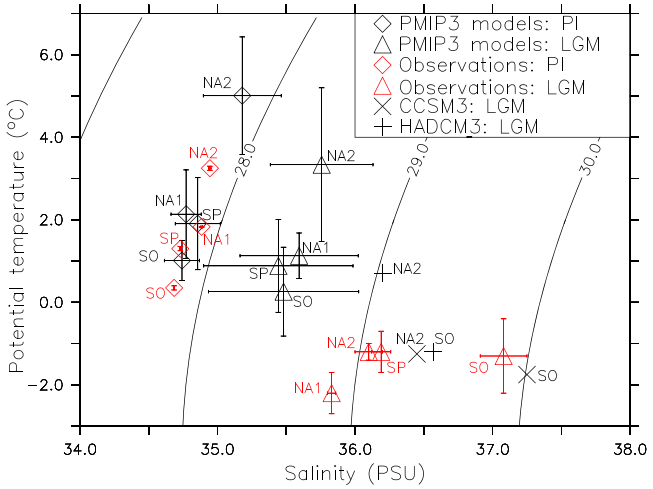

Figure 2. Bottom potential temperature-salinity diagram for the PMIP3 multimodel average (in PIC and LGM simulations), modern observations, and LGM reconstructions from *Adkins et al.* [2002] for two sites in the North Atlantic, one in the South Pacific and one in the Southern Ocean (Atlantic sector). Also included are two LGM PMIP2 models that showed similarities with reconstructions, taken from *Otto-Bliesner et al.* [2007]. Error bars in the multimodel averages are 1σ standard deviations. Contours are potential density in kg/m^3.

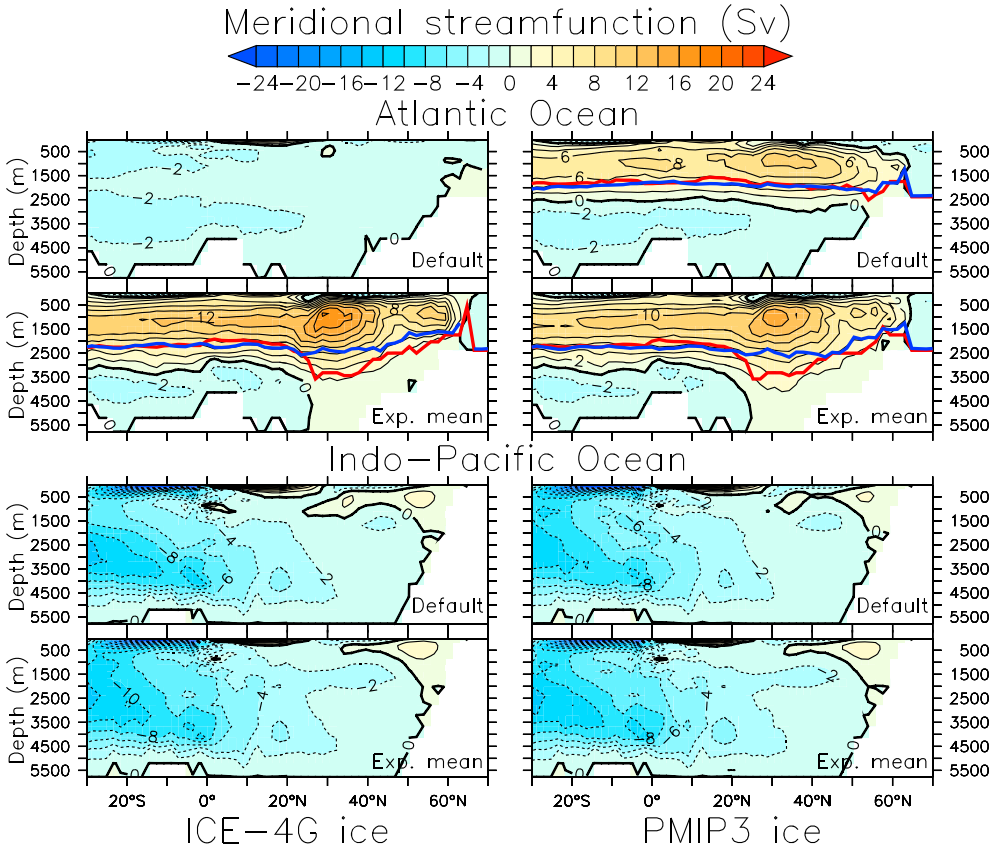

Figure 3. LGM meridional stream function calculated by UVic. (left column) Runs using the ICE-4G LGM land ice reconstruction. (right column) Runs using the PMIP3 LGM land ice reconstruction. Default cases use present-day wind stress obtained from NCEP reanalysis. The experiment mean is the average between runs where PMIP3 LGM anomalies are added to NCEP wind stress. Red and blue lines are as in Figure 1. Note that the AMOC collapses in the default ICE-4G case.

For the PMIP2 experiments (Figure S8 and Table S1), we find an increment in the AMOC in three cases (CCSM3, the Model for Interdisciplinary Research on Climate (MIROC) and the Flexible Global Ocean-Atmosphere-Land System model (FGOALS)) but no change in one case (Centre National de Recherches Météorologiques model (CNRM)). CNRM exhibits smaller changes in wind stress over the NA than the other models, which could be the reason behind the discrepant result.

Table 2. Maximum Meridional Overturning, Percentage of Increment Between Wind Stress Experiments and Default Run, Salt Flux F_{salt} in the Atlantic Ocean, and Depth of the AMOC (All at 25°N) in the UVic Model Experiments[a]

Model Case	AMOC (Sv)	Change (%)	F_{salt} (10^6 kg/s)	AMOC Depth (m)	Change (%)
Default	9.10	-	89.23	1905	-
CCSM4	13.56	49	99.32	3103	63
GISS	11.07	22	108.60	2203	16
CNRM	11.15	22	106.10	3300	73
MPI	12.13	33	102.70	3080	62
MIROC	13.33	46	98.78	3060	61
MRI	13.55	49	101.00	3068	61
FGOALS	13.84	52	97.77	3048	60
IPSL	12.78	40	96.60	3123	64

[a]Each row corresponds to wind stress anomalies from a different PMIP3 model. The top row corresponds to the default case. All numbers correspond to experiments using the PMIP3 ice sheet.

4. Discussion

PMIP3 models predict a strengthening and deepening of the AMOC in the LGM. The UVic model produces a similar result, when forced with LGM wind stress anomalies calculated by the same models.

The zonal component of the PMIP3 wind stress anomaly fields exhibits a conspicuous maximum in the NA region (Figure S1). This is an effect of the Laurentide Ice Sheet over North America, which produces stronger and southward shifted westerly winds over the NA.

We hypothesize that the increment in the AMOC strength is controlled by stronger westerly winds over the North Atlantic, which increase the northward salt transport. Resulting higher salinities increase the density of surface waters and intensify deep water formation at high latitudes. This hypothesis is confirmed by analysis of the meridional salt flux F_{salt} at 25°N in the Atlantic, defined as

$$F_{salt} = \int_{25°N}^{90°N} \int_{x_1(y)}^{x_2(y)} (P + R - E)\, dx dy, \quad (1)$$

where E is evaporation, P is precipitation, and R is river discharge (expressed in kg/(m^{2}s)). Table 2 shows that values of F_{salt} are positive at 25°N, indicating a northward salt transport across that latitude. The magnitude in the default simulation is smaller than the ones obtained with any of the PMIP3 wind stress anomalies. There is more salty water being transported northward in the cases with higher wind stress over the NA.

To further test our hypothesis of a NA-driven strengthening of the AMOC in the PMIP3 models, we performed simulations with a multimodel average of the wind stress anomalies, in which we applied the LGM wind stress anomaly only in one hemisphere (Figure S9, left column). We label $\Delta\tau_{SH}$ ($\Delta\tau_{NH}$) the case in which it was applied in the Southern (Northern) Hemisphere. We also performed a simulation using the average anomaly in both hemispheres, referred to as full case.

The AMOC in the default case (Figure S9a) is similar (in values and structure) to that of $\Delta\tau_{SH}$ (Figure S9b), while the AMOC in the full case (Figure S9d) is similar to that of $\Delta\tau_{NH}$ (Figure S9c), indicating that the differences in the AMOC between PIC and LGM simulations is a response to wind stress anomalies in the Northern Hemisphere.

When using LGM wind stress anomalies from the PMIP2 models, the resulting UVic simulated AMOC has in some cases a different sign of change compared to the AMOC from the PMIP2 models (see *Otto-Bliesner et al.* [2007] for AMOC plots of different PMIP2 models and compare to Figure S8 of this work). This suggests that changes in buoyancy forcing are more important in these models. For example, the CCSM3 model used in *Otto-Bliesner et al.* [2007] predicts a weakening of the AMOC in the LGM, even though the transport of the Gulf Stream increases due to wind effects, indicating that changes in buoyancy fluxes decrease the AMOC and dominate wind stress effects. The strong effect of buoyancy in these models is also demonstrated in their bottom salinity values, with a salty SO water, indicating high production of AABW (Figure 2).

Our results are consistent with the results from ocean-atmosphere models, which show a stronger AMOC as a response to increases in ice sheet height [*Otto-Bliesner et al.*, 2006; *Ullman et al.*, 2014; *Zhang et al.*, 2014]. Our simulations suggest that enhanced wind-driven salt transport may, at least partly, explain this response.

Because of the similarity between PMIP3 models' outputs and our wind stress experiments with the UVic model, our results suggest that in the PMIP3 case, wind stress plays a fundamental part in the LGM-PIC AMOC differences and that changes in buoyancy fluxes play a smaller role. This is in contrast to the response in CCSM3 and UVic model, where changes in buoyancy fluxes, which tend to decrease the AMOC (Figure S6), are similar but slightly larger than the effects of the PMIP3 wind stress (Figure 3).

5. Conclusions

UVic model responds very consistently with a strengthening and deepening of the AMOC when forced with LGM wind stress anomalies from PMIP models. Our analysis suggests that stronger wind stress over the NA due to the effects of the Laurentide Ice Sheet on atmospheric circulation causes enhanced northward salt transport in an intensified gyre circulation. This is an important process explaining the LGM-PIC differences predicted by these models. The result represents an improvement in our understanding of the mechanics governing the LGM AMOC in climate models. The fact that the results are robust across all models examined

suggests that this process may also play an important role in the real world, confirming the speculation by *Wunsch* [2003].

It will be an important task for future work to resolve the apparent inconsistency between PMIP models' LGM circulation and reconstructions. This inconsistency casts doubt on future AMOC projections with these models [e.g., *Weaver et al.*, 2012]. One possible explanation may be that not all PMIP3 models were in equilibrium [*Zhang et al.*, 2013].

Since LGM wind stress, closure of Bering Strait [*Hu et al.*, 2010], and increased tidal mixing [*Schmittner et al.*, 2015] all tend to increase the strength and depth of the AMOC, a countering effect has to be invoked to reproduce observations of a weaker and shallower overturning during the LGM.

Changes in buoyancy fluxes, as suggested by CCSM3 and the UVic model, are a good candidate. A detailed analysis of the PMIP3 models' buoyancy fluxes and their effects on the AMOC remains to be performed. *Ferrari et al.* [2014] have recently hypothesized that the expansion of Antarctic sea ice explains the shoaling of the AMOC. However, since the PMIP models do simulate more extensive sea ice, this process appears to be not very important in these models. We conclude that the specific mechanism for the required buoyancy flux changes remains elusive.

Finally, due to the high consistency between model results, we do not rule out the possibility that some proxies may need reinterpretation. To study the implications of the modeled LGM circulation on isotope distributions will be useful for a more direct comparison.

Acknowledgments

This study was supported by NSF's Marine Geology and Geophysics program (grants OCE-1131834 and OCE-1235544). We acknowledge World Climate Research Programme's Working Group on Coupled Modelling responsible for CMIP, and we thank climate modeling groups for producing and making available their model output. For CMIP the U.S. Department of Energy's PCMDI provides coordinating support and led to the development of software infrastructure in partnership with the Global Organization for Earth System Science Portals. We also want to thank Ricardo Matano and four anonymous reviewers for their suggestions that helped to improve this paper.

References

Abe-Ouchi, A., et al. (2015), Ice-sheet configuration in the CMIP5/PMIP3 Last Glacial Maximum experiments, *Geosci. Model Dev. Discuss.*, *8*(6), 4293–4336.

Adkins, J. F., K. McIntyre, and D. P. Schrag (2002), The salinity, temperature, and δ18O of the glacial deep ocean, *Science*, *298*(5599), 1769–1773.

Braconnot, P., et al. (2007), Results of PMIP2 coupled simulations of the Mid-Holocene and Last Glacial Maximum — Part 1: Experiments and large-scale features, *Clim. Past*, *3*, 261–277.

Braconnot, P., S. P. Harrison, M. Kageyama, P. J. Bartlein, V. Masson-Delmotte, A. Abe-Ouchi, B. Otto-Bliesner, and Y. Zhao (2012), Evaluation of climate models using palaeoclimatic data, *Nat. Clim. Change*, *2*(6), 417–424.

Clark, P. U., A. S. Dyke, J. D. Shakun, A. E. Carlson, J. Clark, B. Wohlfarth, J. X. Mitrovica, S. W. Hostetler, and A. M. McCabe (2009), The Last Glacial Maximum, *Science*, *325*(5941), 710–714.

Ferrari, R., M. F. Jansen, J. F. Adkins, A. Burke, A. L. Stewart, and A. F. Thompson (2014), Antarctic sea ice control on ocean circulation in present and glacial climates, *Proc. Natl. Acad. Sci. U.S.A.*, *111*(24), 8753–8758.

Gebbie, G. (2014), How much did Glacial North Atlantic Water shoal?, *Paleoceanography*, *29*, 190–209, doi:10.1002/2013PA002557.

Gherardi, J.-M., L. Labeyrie, S. Nave, R. Francois, J. F. McManus, and E. Cortijo (2009), Glacial-interglacial circulation changes inferred from 231Pa/230Th sedimentary record in the North Atlantic region, *Paleoceanography*, *24*, PA2204, doi:10.1029/2008PA001696.

Hu, A., G. A. Meehl, B. L. Otto-Bliesner, C. Waelbroeck, W. Han, M.-F. Loutre, K. Lambeck, J. X. Mitrovica, and N. Rosenbloom (2010), Influence of Bering Strait flow and North Atlantic circulation on glacial sea-level changes, *Nat. Geosci.*, *3*(2), 118–121.

Kalnay, E., et al. (1996), The NCEP/NCAR reanalysis 40-year project, *Bull. Am. Meteorol. Soc.*, *77*(3), 437–471.

Kuhlbrodt, T., A. Griesel, M. Montoya, A. Levermann, M. Hofmann, and S. Rahmstorf (2007), On the driving processes of the Atlantic meridional overturning circulation, *Rev. Geophys.*, *45*, RG2001, doi:10.1029/2004RG000166.

Lippold, J., Y. Luo, R. Francois, S. E. Allen, J. Gherardi, S. Pichat, B. Hickey, and H. Schulz (2012), Strength and geometry of the glacial Atlantic Meridional Overturning Circulation, *Nat. Geosci.*, *5*(11), 813–816.

Lynch-Stieglitz, J., W. B. Curry, and N. Slowey (1999), Weaker Gulf Stream in the Florida Straits during the Last Glacial Maximum, *Nature*, *402*(6762), 644–648.

Lynch-Stieglitz, J., et al. (2007), Atlantic meridional overturning circulation during the Last Glacial Maximum, *Science*, *316*(5821), 66–69.

McCarthy, G., D. Smeed, W. Johns, E. Frajka-Williams, B. Moat, D. Rayner, M. Baringer, C. Meinen, J. Collins, and H. Bryden (2015), Measuring the Atlantic meridional overturning circulation at 26°N, *Prog. Oceanogr.*, *130*, 91–111.

McManus, J., R. Francois, J.-M. Gherardi, L. Keigwin, and S. Brown-Leger (2004), Collapse and rapid resumption of Atlantic meridional circulation linked to deglacial climate changes, *Nature*, *428*(6985), 834–837.

Montoya, M., and A. Levermann (2008), Surface wind-stress threshold for glacial Atlantic overturning, *Geophys. Res. Lett.*, *35*, L03608, doi:10.1029/2007GL032560.

Oka, A., H. Hasumi, and A. Abe-Ouchi (2012), The thermal threshold of the Atlantic meridional overturning circulation and its control by wind stress forcing during glacial climate, *Geophys. Res. Lett.*, *39*, L09709, doi:10.1029/2012GL051421.

Otto-Bliesner, B. L., C. Hewitt, T. Marchitto, E. Brady, A. Abe-Ouchi, M. Crucifix, S. Murakami, and S. Weber (2007), Last Glacial Maximum ocean thermohaline circulation: PMIP2 model intercomparisons and data constraints, *Geophys. Res. Lett.*, *34*, L12706, doi:10.1029/2007GL029475.

Otto-Bliesner, B. L., E. C. Brady, G. Clauzet, R. Tomas, S. Levis, and Z. Kothavala (2006), Last Glacial Maximum and Holocene climate in CCSM3, *J. Clim.*, *19*(11), 2526–2544.

Peltier, W. R. (2004), Global glacial isostasy and the surface of the ice-age Earth: The ICE-5G (VM2) model and GRACE, *Annu. Rev. Earth Planet. Sci.*, *32*, 111–149.

Peltier, W. R. (1994), Ice age paleotopography, *Science*, *265*, 195–195.

Schmittner, A., and G. Egbert (2013), An improved parameterization of tidal mixing for ocean models, *Geosci. Model Dev.*, *7*, 211–224.

Schmittner, A., J. Green, and S. Wilmes (2015), Glacial ocean overturning intensified by tidal mixing in a global circulation model, *Geophys. Res. Lett.*, *42*, 4014–4022, doi:10.1002/2015GL063561.

Stocker, T. F., et al. (2013), Climate change 2013: The physical science basis. Working Group I contribution to the fifth assessment report of the Intergovernmental Panel on Climate Change-abstract for decision-makers, *Tech. Rep.*, Groupe d'experts intergouvernemental sur l'evolution du climat/Intergovernmental Panel on Climate Change–IPCC, C/O WMO, 7bis Avenue de la Paix, Geneva, Switzerland.

Toggweiler, J., and B. Samuels (1995), Effect of Drake Passage on the global thermohaline circulation, *Deep Sea Res., Part I*, *42*(4), 477–500.

Ullman, D., A. LeGrande, A. Carlson, F. Anslow, and J. Licciardi (2014), Assessing the impact of Laurentide Ice Sheet topography on glacial climate, *Clim. Past*, *10*, 487–507.

Weaver, A. J., et al. (2001), The UVic Earth System Climate Model: Model description, climatology, and applications to past, present and future climates, *Atmos. Ocean*, *39*(4), 361–428.

Weaver, A. J., et al. (2012), Stability of the Atlantic meridional overturning circulation: A model intercomparison, *Geophys. Res. Lett.*, *39*, L20709, doi:10.1029/2012GL053763.

Weber, S., S. Drijfhout, A. Abe-Ouchi, M. Crucifix, M. Eby, A. Ganopolski, S. Murakami, B. Otto-Bliesner, and W. Peltier (2007), The modern and glacial overturning circulation in the Atlantic Ocean in PMIP coupled model simulations, *Clim. Past*, *3*(1), 51–64.

Wunsch, C. (2003), Determining paleoceanographic circulations, with emphasis on the Last Glacial Maximum, *Quat. Sci. Rev.*, *22*(2), 371–385.

Zhang, X., G. Lohmann, G. Knorr, and X. Xu (2013), Different ocean states and transient characteristics in Last Glacial Maximum simulations and implications for deglaciation, *Clim. Past*, *9*, 2319–2333.

Zhang, X., G. Lohmann, G. Knorr, and C. Purcell (2014), Abrupt glacial climate shifts controlled by ice sheet changes, *Nature*, *512*(7514), 290–294.